Diencephalic Pediatric Low-grade Glioma Harboring the BRAF V600E Mutation Presenting with Various Morphologies in Sequential Biopsy Specimens

Yukitomo Ishi, MD[1]; nekozamurai@me.com

Kanako C. Hatanaka, MD[2]; kyanack@huhp.hokudai.ac.jp

Shigeru Yamaguchi, MD[1]; yama-shu@med.hokudai.ac.jp

Hiromi Fujita, MD[2]; hiris@wb4.so-net.ne.jp

Hiroaki Motegi, MD[1]; moccihiro@yahoo.co.jp

Hiroyuki Kobayashi, MD[1]; hiro-ko@med.hokudai.ac.jp

Shunsuke Terasaka, MD[1]; terasas@med.hokudai.ac.jp

Kiyohiro Houkin, MD[1]; houkin@med.hokudai.ac.jp

[1]Department of Neurosurgery, Hokkaido University School of Medicine

[2]Department of Surgical Pathology, Hokkaido University Hospital

Corresponding Author:

Shigeru Yamaguchi, MD

Department of Neurosurgery

Hokkaido University Graduate School of Medicine

North 15 West 7, Kita-ku, Sapporo 060-8638, Japan

Phone: (+81)11-706-5987

Fax: (+81)11-708-7737

E-mail: yama-shu@med.hokudai.ac.jp

Abstract

A 5-year-old boy underwent biopsy of an intra-axial calcified tumor in the hypothalamus, which was incidentally found. Based on the presence of ganglion-like cells combined with glial cell element, the pathological diagnosis was ganglioglioma. Because the tumor grew gradually in size over the next 2 years, he underwent chemotherapy with temozolomide. However, at 8 years of age, the boy developed hydrocephalus and the cystic lesion had re-grown. Endoscopic cyst fenestration and tumor biopsy was performed, and pathological diagnosis was tentatively oligodendroglioma based on the presence of tumor cells with a perinuclear halo. At 10 years of age, hydrocephalus recurred and the cystic lesion had re-grown. A second round of endoscopic cyst fenestration and tumor biopsy led to a pathological diagnosis of pilocytic astrocytoma due a biphasic appearance with areas of dense tumor cells and microcystic areas, tumor cells with eosinophilic processes, and the presence of an eosinophilic granular body. Genetic analysis of the first biopsy successfully identified the *BRAF V600E* mutation. Because pathological diagnosis of diencephalic low-grade glioma harboring *BRAF V600E* would be sometimes difficult due to pathological variations, pathological diagnosis should be performed under the consideration of molecular diagnosis of *BRAF V600E* for optimal diagnosis and treatment.

(198/200 words)

Key words: BRAF 600E; glioma; pilocytic astrocytoma; ganglioglioma; oligodendroglioma

Abbreviations used in this paper: CT = computed tomography; GG = ganglioglioma; Gd = gadolinium; GFAP = glial fiber acid protein; GTR = gross total resection; HE = hematoxylin and eosin; LGG = low-grade glioma; MRI = magnetic resonance imaging; OL = oligodendroglioma; PA = pilocytic astrocytoma; PLGG = pediatric low-grade glioma; PMA = pilomyxoid astrocytoma; TMZ = temozolomide; WI = weighted image

Introduction

A missense mutation at amino acid position 600 of the *BRAF* oncogene (*BRAF V600E*), which changes a valine residue into a glutamate residue, is frequently detected in pediatric low-grade gliomas (PLGGs), including 18%–38.7% of ganglioglioma cases (GG) [1-3], 9%–15.6% of pilocytic astrocytoma cases (PA) [1-3] and 50%–66.7% of pleomorphic xanthoastrocytoma cases [1-4]. Activation of the mitogen-activated protein kinase (MAPK)/extracellular signal-regulated kinase (ERK) pathway caused by mutated BRAF protein is considered to be a primary causative mechanism in the development of these tumors [5].

PA is the most common histological type of glioma found in children [6]. Typical pathological findings of PA include low to moderate cellularity with compact, densely fibrillated areas rich in Rosenthal fibers as well as loosely textured areas composed of multipolar cells [6]. However, the pathological diagnosis of PA is sometimes difficult because of histological variations involving oligodendroglioma-like cells [6, 7] or ganglion-like cells [8]. GG is a brain tumor that is classified as WHO grade 1 and preferentially occur in children or young adults [9]. The histopathological hallmark of GG is a combination of neuronal and glial cell elements, but the glial component shows variability and eosinophilic granular bodies, Rosenthal fibers, myxoid degeneration or clear-cell morphology that resembles PA or oligodendroglioma would be frequently observed [9]. Therefore, definitive diagnosis of PA or GG is sometimes difficult in pathological examinations of the biopsy specimens [6]. Here, we present a case of PLGG harboring the *BRAF V600E* mutation in which the patient received surgical intervention on three occasions; on each intervention, biopsied tissue revealed different pathological findings.

Clinical summary

This case involved a boy in whom a cerebral mass had been incidentally detected by computed tomography (CT) in a previous hospital following a head injury at three years of age. Twenty-nine months later, at the age of 5 years old, he was referred to our institution because serial radiological follow-up had shown that the lesion had been growing gradually. Head CT (Fig. 1a, b) showed apparent calcification in the left basal ganglia. Magnetic resonance imaging (MRI, Fig. 1c–f) detected an intra-axial tumor with a cystic component infiltrating into the left cerebral hemisphere. The tumor was mainly located in the left hypothalamus, basal ganglia, and temporal lobe. The tumor showed mixed-high intensity on both T1- and T2-weighted images (WI) and was heterogeneously enhanced by gadolinium contrast medium. Open biopsy was performed via left fronto-temporal craniotomy upon the tumor bulging out to the basal

cistern. Pathological diagnosis at this point in time was GG (Fig.2). The patient was discharged from hospital without postoperative complications. Considering previous progression and unresectability of the tumor, avoidance of irradiation and request from patients, he underwent oral administration of temozolomide (TMZ). Thirty months later, at the age of 8 years, he complained of progressive headache. MRI (Fig. 3a) revealed enlargement of the cystic lesion of the tumor and subsequent obstructive hydrocephalus. He then underwent endoscopic cyst fenestration and tumor biopsy (VISERA Ventricular Videoscope VEF-V, Olympus, Tokyo, Japan) via the anterior horn of the left lateral ventricle. Pathological diagnosis (Fig. 3b-g) at this stage was tentatively oligodendroglioma (OL). Oral administration of TMZ was continued for an additional 11 months. Twelve months after TMZ therapy had ceased, at the age of 10 years, follow-up MRI (Fig. 4a) revealed that the cystic lesion had regrown and that hydrocephalus had recurred. Endoscopic cyst fenestration and tumor biopsy was performed again via the same route as previously. On this occasion, pathological diagnosis (Fig. 4b-i) was PA. He was subsequently discharged from hospital without additional treatment, but underwent a ventriculo-peritoneal shunt six months later because of the recurrence of hydrocephalus. At the time of writing, the patient is still alive and enjoying a normal education, despite the fact that it is now 105 months since his initial presentation.

Pathological findings

Biopsy specimen obtained at the first operation

Hematoxylin and eosin (HE) staining presented ganglion-like cells harboring a prominent nucleoli and spindle-shaped tumor cells with small nuclei (Fig. 2a, b). There were some calcifications. Mitosis, necrosis or microvascular proliferation were not seen. Upon immunohistochemical staining, spindle-shaped cells between neuron-like cells were positive for glial fibrillary acidic protein (GFAP, Fig. 2c). Ganglion-like cells were positive for Neurofilament (Fig.2d) but negative for GFAP (Fig.2c) and Olig2. Neurofilament was also positive in the background (Fig2c). Ki-67 labeling index was approximately 3.0%. Although binucleated neurons or perivascular cuffing were not observed in the specimen, the tumor was diagnosed as ganglioglioma considering the heterogeneous combination of ganglion-like cells and glial cell elements at that time.

Biopsy specimen obtained at the second operation

HE staining presented tumor cells with round to oval-shaped nuclei and a perinuclear halo, together with spindle-shaped cells with small nuclei (Fig. 3b,c). Ganglion-like cells were not observed. There were some calcifications. Upon immunohistochemical staining, tumor cells were positive for GFAP and Olig-2 but negative for Neurofilament. Ki-67 labeling index was 4.2%. 1p/19q co-deletion was not detected by fluorescence *in situ* hybridization. At the diagnosis, the first biopsied specimen was reviewed, but it was considered that the histological feature was different from the first one. Although typical honeycomb appearance or chicken-wire network were not observed, the tumor was diagnosed as tentatively "oligodendroglioma" considering the morphology of tumor cells harboring perinuclear halo-like structure at that time.

Biopsy specimen obtained at the third operation

HE staining showed a biphasic appearance with areas of dense tumor cells and microcystic areas (Fig. 4b). In the area showing dense tumor cells, it was evident that the tumor cells exhibited nuclei that were large and oval (Fig. 4c), thus resembling the tumor cells retrospectively observed in specimens obtained from the second operation. In the microcystic area, tumor cells exhibited a round or spindle-shaped nucleus with eosinophilic processes (Fig. 4d). Eosinophilic granular bodies (Fig. 4d) and Rosenthal fibers (Fig. 4e) were also observed. Immunohistochemical staining showed that tumor cells were positive for GFAP and Olig-2 and negative for Neurofilament and NeuN. Ki-67 labeling index was approximately 3.3%. Pathological diagnosis was pilocytic astrocytoma considering typical findings such as biphasic pattern and eosinophilic granular bodies.

Reconsideration of pathological findings thorough all specimens

Because pathological diagnosis differed in each specimen, we reviewed pathological findings in each specimen. HE staining of the first specimen contained tumor piloid cells with hairy cellular processes (Fig.2b), although it did not occupied major region, that suggest the diagnosis of PA. Such tumor cells were also observed in the second specimen (Fig.3c). Overall, the first and second histological features were considered as some parts of PA. Additional immunohistochemical studies were performed in the first specimen. CD34 was negative. NeuN was negative for Ganglion-like cells. The possibility was remained that these ganglion-like cells were dysplastic neuron because they were positive for Neurofilament, chromogranin-A and synaptophysin, but negative for NeuN.

Genetic analysis

Genetic analysis, which was performed after the third operation, was carried out using the frozen specimen obtained from the first biopsy. Using extracted DNA and RNA from this specimen, we specifically investigated the fusion gene between *KIAA1549* and *BRAF* (*K-B* fusion) by reverse transcription (RT)-PCR, and missense mutations at *BRAF V600*, *H3F3A K27/G34*, *IDH1 R132*, *IDH2 R172* and within the *TERT* promoter C250/C228 by direct Sanger sequence. The method for sequencing analysis is described in the Supplementary material. Of the genes screened, we successfully detected the *BRAF V600E* mutation (Fig. 2f); no other genetic aberrations were identified.

Discussion

During the routine pathological examination of PA, it is sometimes the case that typical pathological findings are accompanied by oligodendroglioma-like cells [6, 7] or ganglion-like cells [8]. While in the pathological examination of GG, variability of glial component, presence of eosinophilic granular body, Rosenthal fibers or microcystic cavities resembling fibrillary astrocytoma, oligodendroglioma or pilocytic astrocytoma are often observed [9]. Because of such histological variations, it would be sometimes difficult to distinct PA and GG pathologically, especially in case with biopsied specimen [6]. Because case of pathological findings in diencephalic low-grade glioma (LGG) in sequential biopsy specimen has been rarely reported, difference of pathological findings in different site or timing of diencephalic LGG is unclear. In the present case, specimen obtained at the first operation was diagnosed as gangliоglioma considering the heterogeneous combination of neuronal and glial cell elements, but the typical findings for PA were observed in the biopsy specimen obtained during the third operation. Two possible diagnoses were considered; PA and GG. In the former diagnosis, specimen with ganglion-like cells would be biopsied at the first operation and specimen with oligodendroglioma-like cells would be biopsied at the second operation. In fact, piloid tumor cells were confirmed at the reconsideration of all 3 different specimens. In the latter diagnosis, oligodendroglioma-like cells was observed at the second specimen and the part where myxoid degeneration and eosinophilic granular bodies were predominant would be observed at the third specimen. Presence of dysplastic neuron suggested by positive Neurofilament and Chromogranin-A supported the diagnosis of GG, but the negative staining for CD34 was not usual for GG [9]. Negative NeuN staining is consistent with either diagnosis of PA and GG [9, 10]. In either diagnosis of PA and GG, oligodendroglioma-like cells can be observed. Because all specimens were obtained by biopsy, it would be difficult to make definitive diagnosis by small biopsy specimens. Therefore we consider the pathological diagnosis of this tumor as unclassified LGG, but the presence of piloid tumor cells suggested the diagnosis of PA most likely. Retrospectively, it

might be difficult to diagnose this tumor as PA because the first and second biopsied specimens include mainly Ganglion-like cells or oligodendroglioma-like element, not “typical” PA. And besides, now oligodendroglioma is diagnosed based on not only histological features but also molecular studies. The second specimen was diagnosed as “oligodendroglioma”, but nowadays we can’t diagnose this specimen as oligodendroglioma.

The majority of PAs, especially those in the cerebellum, are known to exhibit the *K-B* fusion [6]. Cases of PA exhibiting the *BRAF V600E* are more frequently found in extra-cerebellar [2] or supratentorial [6] lesions; and especially in 33% of diencephalic PAs [2]. PLGG in the diencephalon, such as PA and pilomyxoid astrocytoma (PMA), exhibiting the *BRAF V600E* mutation is clinically distinct from cases that do not possess *BRAF V600E* [5]. Gangliоglioma is also one of the major PLGGs in which *BRAF V600E* is frequently detected [1-3]. GG can occur throughout the central nervous system [9], however the majority of PLGG arising in the diencephalon have been diagnosed as PA or PMA[5]. Although genetic analysis could not make definitive diagnosis in this case because *BRAF V600E* can be detected both in PA and GG, previous report indicated that diencephalic LGG harboring *BRAF V600E* tend to lack the classical pathological features upon initial diagnosis [5], which suggest the difficulty of pathological diagnosis of PLGG harboring *BRAF V600E*. As in present case, LGG harboring *BRAF V600E* would tend to present various pathological findings due to the site or timing of resection. Therefore, we consider that molecular diagnosis is useful for correct diagnosis of diencephalic LGG especially in case harboring *BRAF V600E*. Moreover, previous report presented the worse prognosis of diencephalic PLGG harboring *BRAF V600E* compared with PLGG harboring wild type *BRAF* [5]. Therefore, genetic analysis of *BRAF V600E* would be useful to understand the biology and to make decision of treatment for such tumors regardless to pathological findings. Not only for diagnostic value, *BRAF* mutation is considered as a potential therapeutic target for gliomas harboring this mutation [11]. Because *BRAF V600E* can be detected by immunohistochemistry with favorable sensitivity and specificity [12], significance of *BRAF V600E* detection would increase in the future.

Conclusions

We reported the case of diencephalic LGG harboring *BRAF V600E* mutation most considered as PA presenting with various pathological findings in 3 sequential biopsy specimens. Although diencephalic LGG harboring *BRAF V600E* is not rare, pathological diagnosis would be sometimes difficult because of the lack of typical pathological findings especially in the diagnosis of small specimen obtained from biopsy surgery. Pathological diagnosis should be performed under the consideration of molecular diagnosis of *BRAF V600E* for optimal diagnosis and treatment in such cases.

Conflict of interest

The authors declare that they have no conflict of interest.

References

[1] Chappe C, Padovani L, Scavarda D et al (2013) Dysembryoplastic neuroepithelial tumors share with pleomorphic xanthoastrocytomas and gangliogliomas BRAF(V600E) mutation and expression. Brain Pathol 23:574-583
[2] Schindler G, Capper D, Meyer J et al (2011) Analysis of BRAF V600E mutation in 1,320 nervous system tumors reveals high mutation frequencies in pleomorphic xanthoastrocytoma, ganglioglioma and extra-cerebellar pilocytic astrocytoma. Acta Neuropathol 121:397-405
[3] Myung JK, Cho H, Park CK et al (2012) Analysis of the BRAF(V600E) Mutation in Central Nervous System Tumors. Transl Oncol 5:430-436
[4] Lee D, Cho YH, Kang SY et al (2015) BRAF V600E mutations are frequent in dysembryoplastic neuroepithelial tumors and subependymal giant cell astrocytomas. J Surg Oncol 111:359-364
[5] Ho CY, Mobley BC, Gordish-Dressman H et al (2015) A clinicopathologic study of diencephalic pediatric low-grade gliomas with BRAF V600 mutation. Acta Neuropathol 130:575-585
[6] Collins VP, Jones DT and Giannini C (2015) Pilocytic astrocytoma: pathology, molecular mechanisms and markers. Acta Neuropathol 129:775-788
[7] Rodriguez FJ, Lim KS, Bowers D et al (2013) Pathological and molecular advances in pediatric low-grade astrocytoma. Annu Rev Pathol 8:361-379[
[8] Burger PC and Scheithauer BW (2007) Tumors of the Central Nervous System. American Registry of Pathology, Washington
[9] Becker AJ WO, Figarella-Branger D, Blumcke I, Capper D (2016) WHO Classification of Tumours of the Central Nervous System. International Agency of Research on Cancer, Lyon
[10] Preusser M, Laggner U, Haberler C et al (2006) Comparative analysis of NeuN immunoreactivity in primary brain tumours: conclusions for rational use in diagnostic histopathology. Histopathology 48:438-444
[11] Dasgupta T, Olow AK, Yang X et al (2016) Survival advantage combining a BRAF inhibitor and radiation in BRAF V600E-mutant glioma. J Neurooncol 126:385-393
[12] Capper D, Preusser M, Habel A et al (2011) Assessment of BRAF V600E mutation status by immunohistochemistry with a mutation-specific monoclonal antibody. Acta Neuropathol 122:11-19

Figure legends

Fig. 1. Radiological examinations upon admission

a. Head computed tomography (CT) presenting a high-density lesion in the left basal ganglia

b. Magnetic resonance imaging (MRI) of T2WI depicting the lesion as high intensity, and showing a cystic component

c. Axial view of gadolinium-enhanced T1WI (Gd-T1WI) depicting heterogeneous enhancement of the lesion

d. Coronal view of Gd-T1WI depicting the lesion extending from the left hypothalamus to the basal ganglia and temporal lobe. Biopsied site at the first operation is indicated (arrow).

Fig. 2. Pathological and genetic examination upon first operation

a, b. Hematoxylin and eosin (HE, original magnification×20 and ×400, respectively) staining showing ganglion-like cells with clear nuclear bodies and spindle-shaped tumor cells with small nuclei. Piloid tumor cells (arrow) are also contained.

c. Immunostaining showed that the cytoplasm of tumor cells was positive for glial fiber acid protein (GFAP)

d. Immunostaining showed strong positive neurofilament staining within the cytoplasm of tumor cells

e. Sanger sequencing of the biopsy specimen obtained during the first operation showed a missense mutation at codon 600 of the *BRAF* oncogene

Fig. 3. Radiological and pathological examination upon second operation

a. Coronal view of preoperative magnetic resonance imaging (MRI) (Gd-T1WI) showing dilatation of the cystic component of the tumor and subsequent obstructive hydrocephalus. The site where endoscopic fenestration and biopsy were performed is indicated by the arrow.

b, c. Hematoxylin and eosin (HE) staining (original magnification×20 and ×400, respectively) showing tumor cells with large and oval-shaped nuclei and perinuclear halos, along with spindle-shaped cells with small nuclei. Piloid tumor cells (arrow) are also contained.

Fig. 4. Radiological and pathological examination upon third operation

a. Coronal View of preoperative magnetic resonance imaging (MRI) (Gd-T1WI) showing the recurrence of dilatation of the cystic component of the tumor and subsequent obstructive hydrocephalus. The site where endoscopic fenestration and biopsy were performed is indicated by the arrow.

b. Hematoxylin and eosin (HE) (original magnification×20) showing a biphasic appearance with regions of dense tumor cells and microcystic areas

c. Hematoxylin and eosin (HE) (original magnification×40) of the dense area of tumor cells with large and oval nuclei, which resembled tumor cells observed in the biopsy specimen obtained at the second operation

d. Hematoxylin and eosin (HE) (original magnification×40) of the microcystic area of tumor cells with round or spindle-shaped nuclei and eosinophilic processes, and eosinophilic granular bodies (arrows)

e. Hematoxylin and eosin (HE) (original magnification×40) showing Rosenthal fiber (arrow)

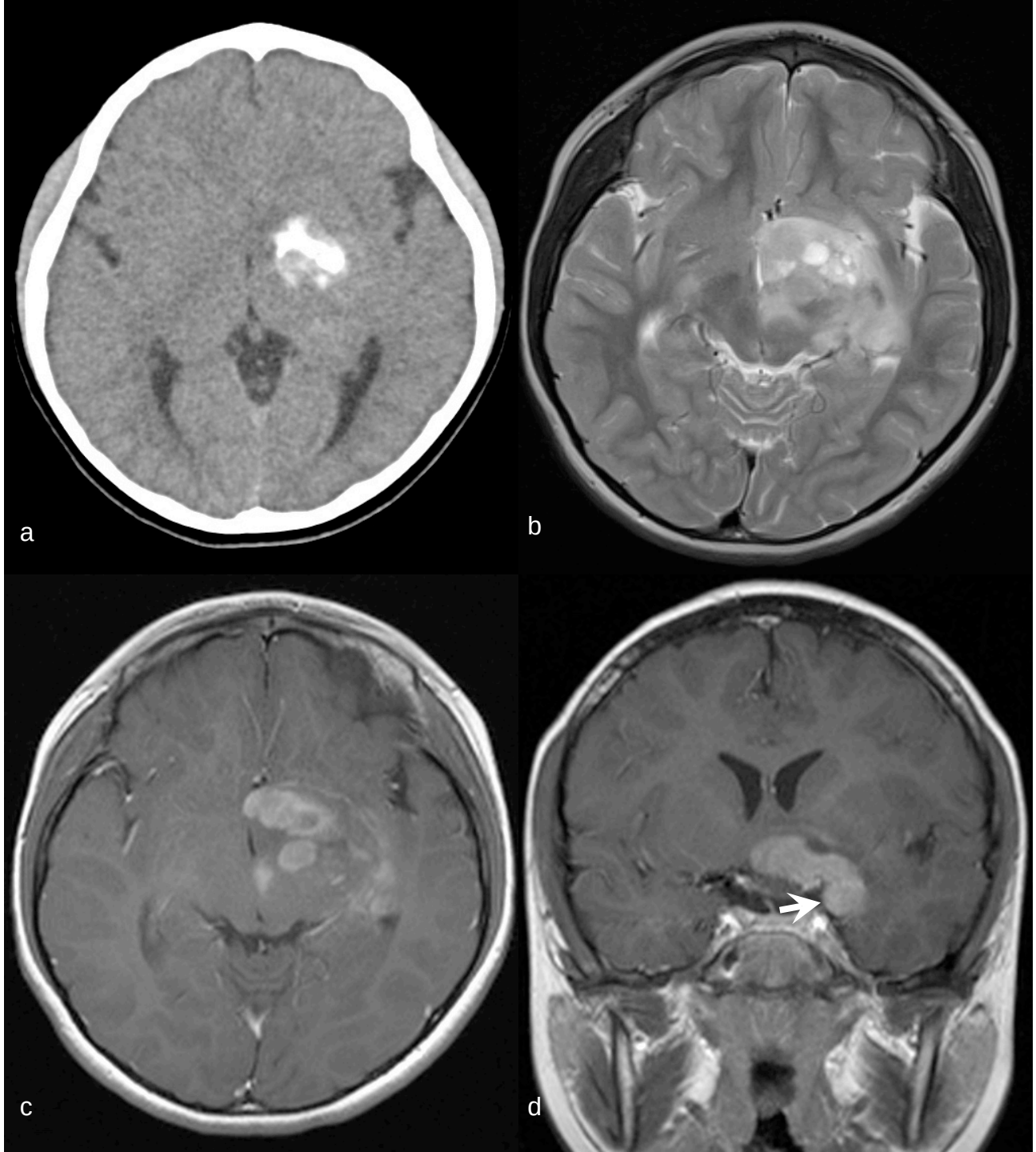

Fig. 1

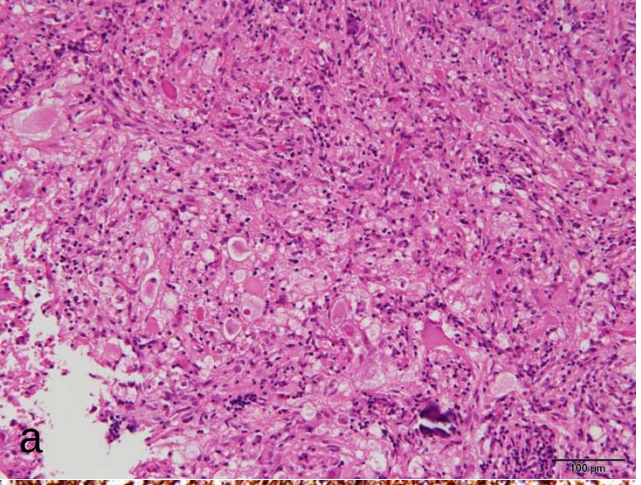

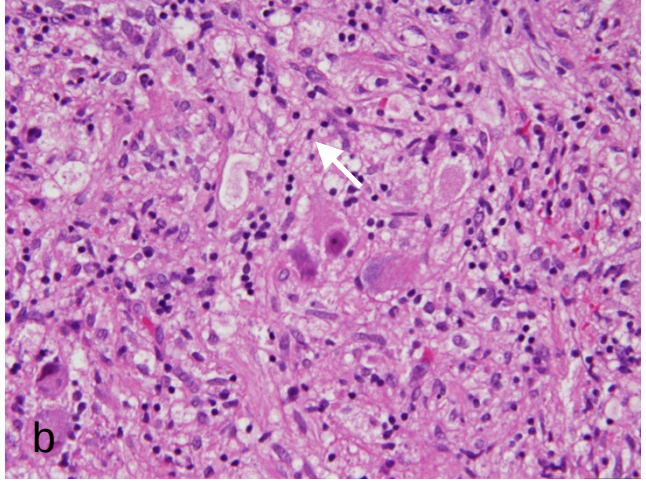

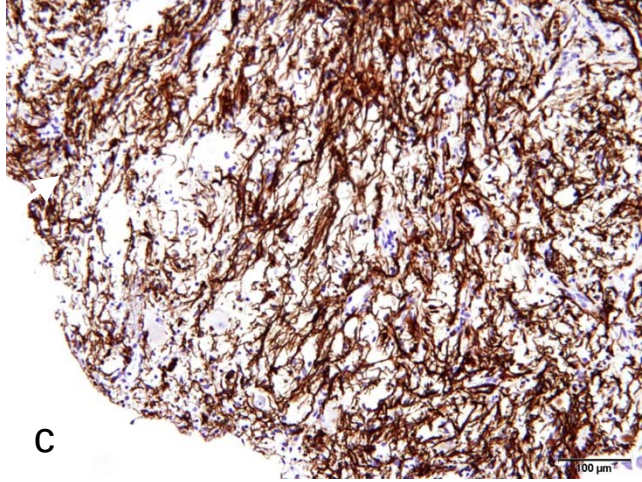

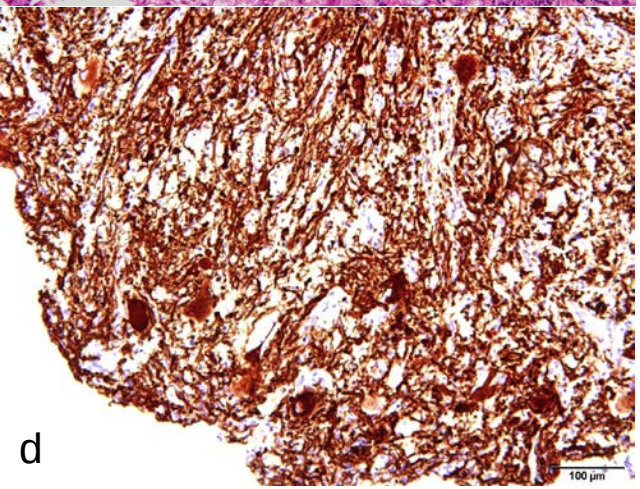

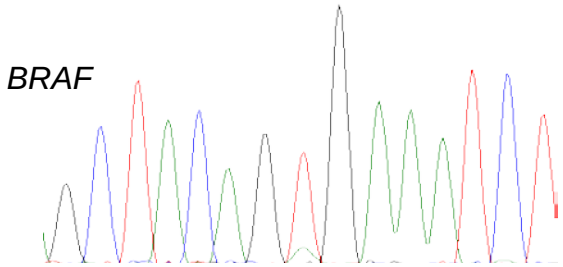

e

c.1799T>A
(V600E)

Fig. 2

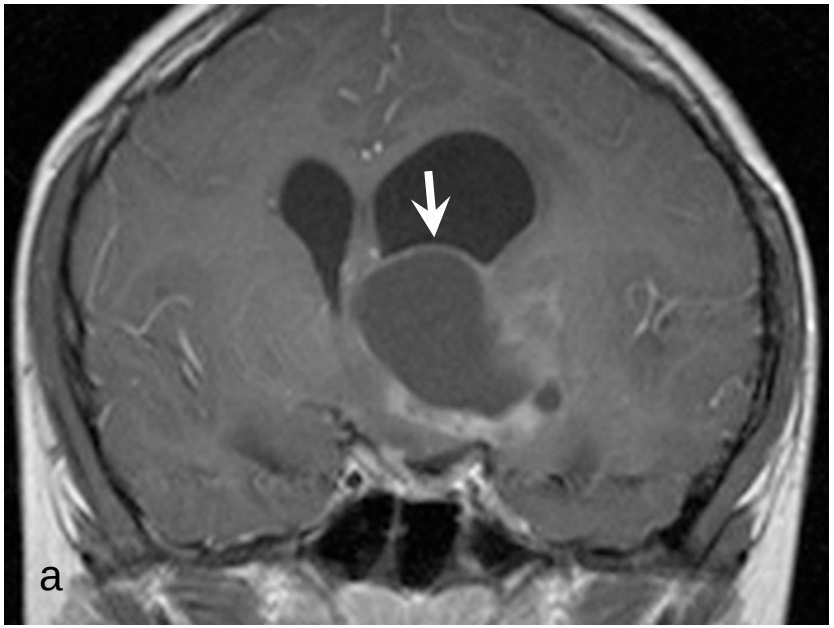

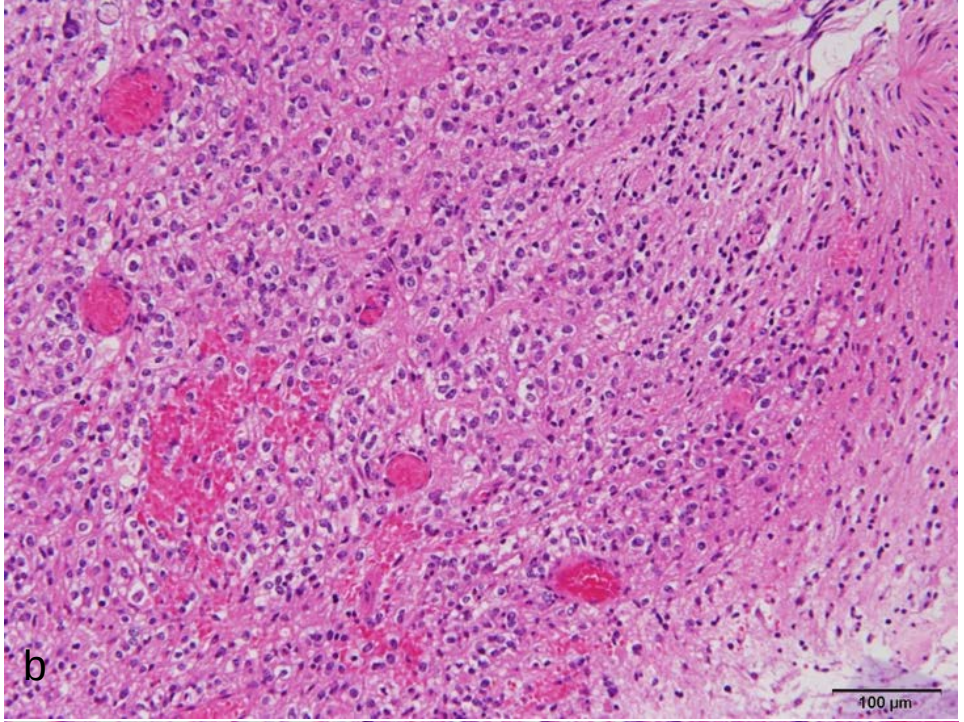

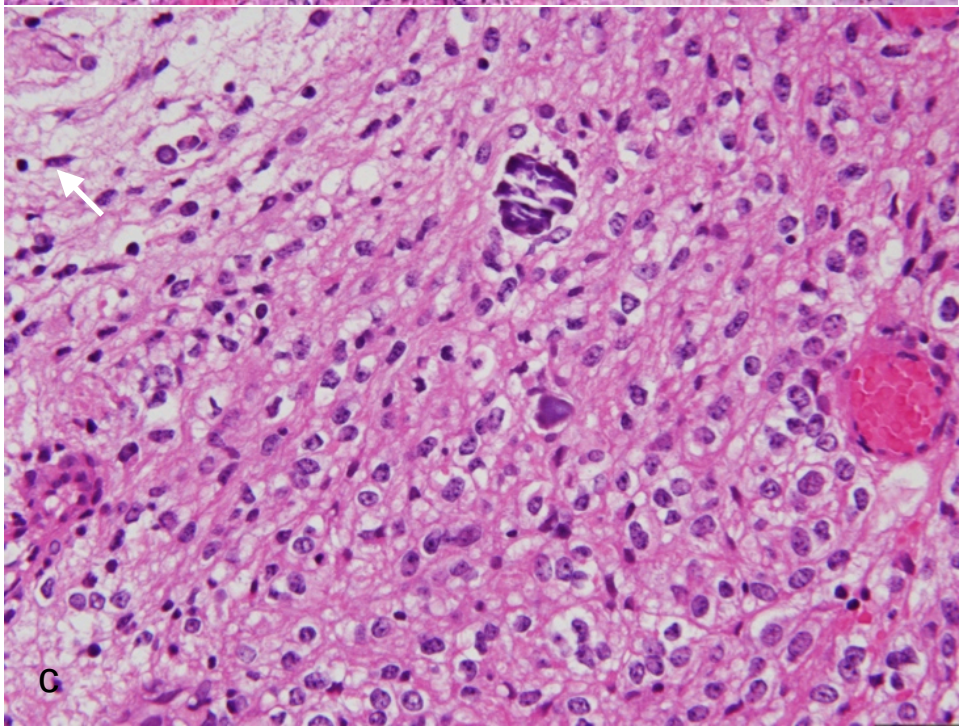

Fig. 3

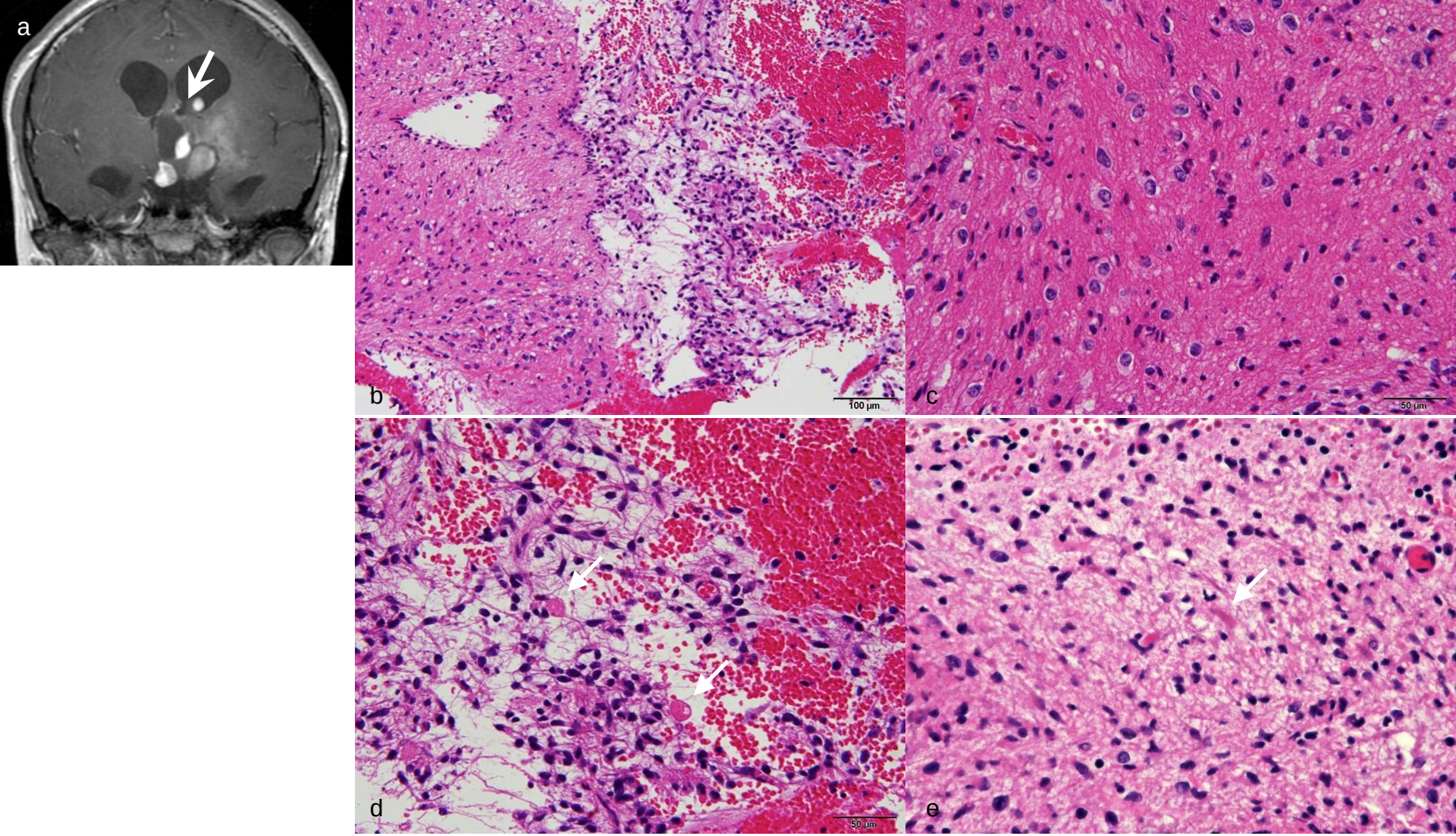

Fig. 4